Toxicology and Applied Pharmacology 334 (2017) 180–191

Contents lists available at ScienceDirect

Toxicology and Applied Pharmacology

journal homepage: www.elsevier.com/locate/taap

HZ-6d targeted HERC5 to regulate p53 ISGylation in human hepatocellular carcinoma

Yang Wang[a,b,c,d], Qi Ding[a,b,c,d], Tao Xu[a,b,c,d], Chang-yao Li[a,b,c,d], Dan-dan Zhou[a,b,c,d], Lei Zhang[a,b,c,d,*]

[a] School of Pharmacy, Anhui Medical University, Hefei 230032, China
[b] Institute for Liver Diseases of Anhui Medical University, Anhui Medical University, Hefei 230032, China
[c] The Key Laboratory of major autoimmune disease, School of Pharmacy, Anhui Medical University, Hefei, Anhui Province 230032,China
[d] The Key Laboratory of Anti-inflammatory and Immune Medicines, Ministry of Education, Anhui Medical University, Hefei, 230032, China

ARTICLE INFO

Keywords:
Hepatocellular carcinoma
HERC5
p53 ISGylation
Disubstituted quinazoline derivative

ABSTRACT

Manipulating the posttranslational modulator of p53 is central in the regulation of its activity and function. ISGylated p53 can be degraded by the 20S proteasome. During this process, HERC5/Ceb1, an IFN-induced HECT-type E3 ligase, mediated p53 ISGylation. In this study, we indicated that HERC5 was over-expressed in both HCC tissue samples and cell lines. Knockdown of HERC5 significantly induced the expression of p53, p21 and Bax/Bcl-2 in HCC cells, resulting in apoptosis augment. Whereas, opposite results were obtained by using HERC5 over-expression. On this basis, we screened a 7, 11-disubstituted quinazoline derivative HZ-6d that could bind to the HERC5 G-rich sequence in vitro. Interestingly, HZ-6d injection effectively delayed the growth of xenografts in nude mice. In vitro, HZ-6d significantly inhibited cell growth, suppressed cell migration, induced apoptosis in HCC cells. Further studies demonstrated the anti-cancer effect of HZ-6d was associated with down-regulation of HERC5 and accumulation of p53. Collectively, we demonstrated that HZ6d is a HERC5 G-quadruplex ligand with anti-tumor properties, an action that may offer an attractive idea for restoration of p53 function in cancers.

1. Introduction

Hepatocellular carcinoma (HCC) is the most common primary malignant tumor of the liver arising from hepatocytes and is considered to be the third leading cause of all cancer-related mortality in the world (Alisi and Balsano, 2007; Jemal et al., 2011). Importantly, the incidence of HCC growth at a rate of about 3–9% annually and approximately 750,000 new confirmed cases of HCC occurs every year (Balogh et al., 2016; Chacko and Samanta, 2016). In spite of advances in the diagnostic techniques and therapeutic strategies of HCC, such as liver transplant, radiation, chemotherapy, or drug combination, the prognosis for HCC patients remains depression (Au and Frenette, 2015; Cherqui, 2015; Abdelsalam et al., 2016). Therefore, a better understanding the mechanism of HCC is needed to discover new therapeutic directions.

All kinds of cancer development arise through the accumulation of genetic mutations and epigenetic modifications, which result in unscheduled and uncontrolled proliferation and growth of normal cells. The tumor suppressor p53, a key guardian of the genome, was first discovered in 1979 (Linzer and Levine, 1979; Levine, 1997). Accumulated data have suggested that p53 gene sequence has been discovered to be absent or mutated in a wide variety of human cancers. The world-wide cancer researchers have pay more attention to target p53 signaling pathway, giving rise to development of a new and hopeful cancer therapy orientation (Chen et al., 2010; Roh et al., 2012; Yue et al., 2013; Bieging et al., 2014; Muller and Vousden, 2014). Emerging evidence have identified p53 is an interferon-stimulated gene 15 (ISG15) target protein (Polyak et al., 1997). ISG15 can covalently modified p53 at 2 sites in the N and C terminus, and ISGylated p53 can be degraded by the 20S proteasome (Huang et al., 2014). Thus, ISG15-dependent modification of p53 may be a promising direction for development of new anti-cancer drugs.

ISG15, an ubiquitin-like protein (UBL), is composed of two tandem repeats of ubiquitin-like domains, which is critical for various target-proteins conjugation (is termed ISGylation) (Loeb and Haas, 1992). Similar to ubiquitination, proteins ISGylation are facilitated by a three-step enzyme system: UBE1L is the first and only ISG15-activating E1 enzyme, UBCH8 as an ISG15-conjugating E2 enzyme and HERC5 as main ISG15 E3 ligase (Kim et al., 2004; Dastur et al., 2006; Wong et al., 2006; Lai et al., 2009). It has been reported that p53 can be modified by

* Corresponding author at: School of Pharmacy, Anhui Medical University, 81 Meishan Road, Hefei, Anhui Province 230032, China.
E-mail address: zhanglei-1@ahmu.edu.cn (L. Zhang).

http://dx.doi.org/10.1016/j.taap.2017.09.011
Received 2 August 2017; Received in revised form 6 September 2017; Accepted 13 September 2017
Available online 15 September 2017
0041-008X/

ISG15. HERC5/Ceb1, an IFN-induced HECT-type E3 ligase, is essential for ISG15 induced p53 degradation (Huang and Bulavin, 2014). Recent data suggested that ISG15 aberrantly expressed in most human tumors (Desai et al., 2008; Cajee et al., 2012; Darb-Esfahani et al., 2014; Li et al., 2014; Desai, 2015; Zuo et al., 2016). However, very little information is available on the role of ISGylation and its enzyme system in HCC.

The G-quadruplex DNA, prominently higher in oncogenic promoter regions, have received much sight in the field of cancer research (Burge et al., 2006; Ma et al., 2015). Our previous studies indicated that a new type of highly selective ligand quinazoline derivatives can bind to and stabilize telomeric G-quadruplex are likely to be effective therapeutics for cancer treatment (Li et al., 2012, 2016b). Then on this basis, we screened a 7, 11-disubstituted quinazoline derivative HZ-6d possessed the activity against a variety of human cancer cell lines (date not shown). Molecular docking and circular dichroism (CD) spectra assay have revealed that HZ-6d could interact with HERC5 G-rich sequence (Adrian et al., 2014), resulting in down-regulation HERC5 expression.

In this research, we investigated the tumor growth suppression of HZ-6d by using transplanted HCC model in nude mice. In vitro, the ISGylation of p53 protein in the development of HCC and the regulatory mechanism of HZ-6d were explored. Our results demonstrated that the anti-neoplasmic activity of HZ-6d probably represents an alternative approach to restore p53 tumor-suppressive function in HCC. Taken together, these data established what we believe to be a new therapeutic rationale for HERC5 inhibition in treatment of ISG15-dependent p53 protein degradation.

2. Materials and methods

2.1. Specimen collection

Tissue samples were collected from the Patients at Department of Surgery and The First Affiliated Hospital of Anhui Medical University (Supplementary Table 1). The research adhered to the standards set by the Declaration of Helsinki. This experiment was approved by the Health Human Research Ethics Committee of Anhui Medical University, and informed consent was obtained from all patients.

2.2. Cell culture and chemical

The Human HepG2 and SMMC-7721 cells and L-02 cell line were cultured in DMEM medium (Hyclone, USA) supplemented with 10% fetal bovine serum (FBS, sijiqing, Hangzhou, Zhejiang, China). All cell cultures were maintained at 37 °C in a humidified incubator at an atmosphere of 5% CO_2. All of the operations provided by approved guidelines. HZ-6d was dissolved in DMSO as 10 mM stock solution, and further diluted with culture medium before it is applied.

2.3. Quantitative real-time PCR

Total RNA was extracted by TRIzol (Invitrogen), and then reverse transcribed to cDNA was performed by a transcriptor first-strand cDNA synthesis kit (TaKaRa, Shiga, Japan). The mRNA relative expression was determined by Real time PCR with SYBR-Green Master Mix (TaKaRa). The GAPDH gene was used an internal control for normalization. The primers used are listed at Supplementary Table 2.

2.4. Western blot analysis

Total proteins were lysed with RIPA buffer (Beyotime, China). Each sample was separated by electrophoresis through 8–12% sodium salt-polyacrylamide gel electrophoresis (SDS-PAGE) and then transferred to polyvinylidene fluoride (PVDF) membrane (Millipore, Billerica, MA, USA). The membranes were incubated with primary antibodies as follows: HERC5, ISG15, p53, p21, Bax and Bcl-2 (Bioss, China) was diluted at 1:300. Caspase3 (Cell Signaling Technology, USA) and β-actin (Bioworld, USA) was diluted at 1:1000. The expression of protein bands were detected by an ECL-chemiluminescent kit (ECL-plus, Thermo Scientific). All of experiments were repeated three to four times independently.

2.5. Small interfering RNA and transfection

Human HepG2 and SMMC-7721 cells were cultured in 6-well plates and were transfected by lipofectamine™2000 (Invitrogen, USA) according to the manufacturer's instruction. The efficiency of transfection was determined by Western blot and quantitative real-time PCR analysis. The oligonucleotide against HERC5 gene or scrambled sequences were designed and synthesized by Gene Pharma Company (Shanghai, China) and contained the follows: HERC5-siRNA (human): 5′-GGAAGGAAAUUUCCCUCAATT-3′, 5′-UUGAGGGAAAUUUCCUUCCTT-3′; and Negative control: 5′-UUCUCCGAACGUGUCACGUTT-3′, 5′-ACGUGACACGUUCGGAGAATT-3′.

2.6. Plasmid construction

The coding region of HERC5 was amplified from human genomic DNA by following primers: Forward: 5′-TACAAGTCCGGACTCAGA TCTATGGAGCGGAGGTCGCGGAGGAA-3′; Reverse: 5′-GTACCGTCGA CTGCAGAATTCGTTGGACAAGCAAGCTGGTC-3′. The amplified products were inserted into the pEGFP-C2 empty vector and were verified by direct DNA sequencing. Cell transfection was performed with lipofectamine™2000 according to the instruction's protocol. The efficiency of over-expression was determined by Western blot and quantitative real-time PCR analysis.

2.7. MTT assay

Proliferation of cell was measured using MTT assay. The cells were seeded on 96-well culture plates, and then add various concentrations of HZ-6d to each well. After cultured 24 h, MTT solution (Invitrogen) was added to each well and the resulting mixture was incubated for 4 h at 37 °C. Finally, 150 μl DMSO was added to each well, and the plates were read at 490 nm wavelength.

2.8. Colony forming assay

For analysis of the effect of HZ-6d on colony forming assay, cells (2000/well) were cultured in 6-well plates with various concentrations of HZ-6d. After two weeks, all plates were treated with 70% ethyl alcohol and stained by 1% crystal violet solution. All results were repeated three to four times independently.

2.9. Cell wound healing assay

Migration of cell was assessed by wound healing assay. After the appropriate treatment, HepG2 and SMMC-7721 cells were cultured in 6-well plate and converged almost 100%, scratched by a yellow pipette tips. Washed the cells with PBS, the medium was changed with DMEM supplemented with 2% FBS. The scratched area was photographed at 0 h and 24 h using light microscope (Olympus, Japan).

2.10. Cell apoptosis assay

Human HepG2 and SMMC-7721 cells were cultured in 6-well plate and treated with various concentration of HZ-6d for 24 h, and then resuspended in the cold PBS buffer. Percentage of apoptotic cells was detected by flow cytometry (BD FACSVerse, USA) using an Annexin-V-FITC Apoptosis Detection Kit (Bestbio, China) according to the manufacturer's instruction exactly.

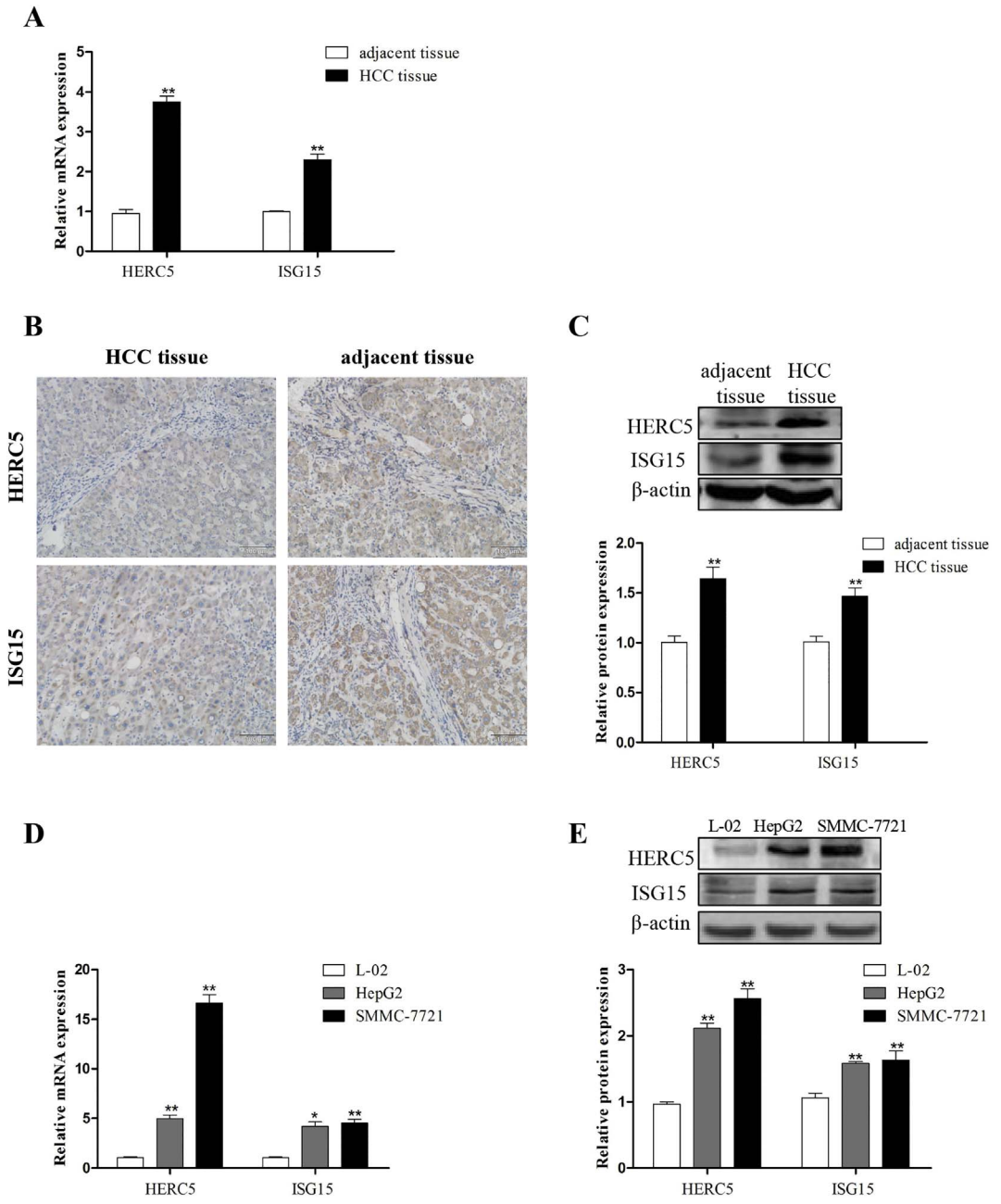

Fig. 1. HERC5 and ISG15 are highly expressed in HCC cells and tissues. (A) The difference in mRNA expression levels of HERC5 and ISG15 in HCC tissues and corresponding adjacent tissues. (B–C) Immunohistochemical and Western blot analysis showed the difference in protein expression levels of HERC5 and ISG15 in the same tissues as described in A. $*p < 0.05$ or $**p < 0.01$ compared with adjacent tissue group ($n = 12$). (D) The mRNA expression levels of HERC5 and ISG15 in normal liver cell line L-02 and HCC cell lines HepG2 and SMMC-7721. (E) Western blot analysis showed the difference in protein expression levels of HERC5 and ISG15 in the same cell lines as described in D. $*p < 0.05$ or $**p < 0.01$ compared with L-02 group. Data are represented as mean ± SD for three independent experiments.

2.11. Molecular modeling

The crystal structure of the parallel-type HERC5 G-quadruplex (PDB: 2MB4) was used as the initial model for investigating the interaction between HZ-6d and HERC5 DNA. Docking studies were carried out using the AUTODOCK 4.0. One hundred independent docking runs were carried out for the ligand. The conformations of the ligand were chosen on the basis of the ligand's optimal binding arrangement with the G-tetrads and the lowest final docked energy.

2.12. CD spectroscopy assay

The HERC5 G-rich sequence d (5′-AGGGGGGAGGGAGGGTGG-3′) oligonucleotide was dissolved in Tris–HCl buffer (10 mM, pH 7.2), containing with or without KCl (100 mM), to obtain a final concentration of 5 μM. The mixed solutions were heated for about 5 min at about 95 °C, slowly cooled to room temperature, cultured at 4 °C overnight. Subsequently, 0.5 s per-point from 220 nm to 450 nm and 1 nm bandwidth were used to record on the spectrophotometer. CD spectra signals were evaluated as the average of two scan and processes data by Origin 8.0 (Origin Lab Corp).

2.13. Animal experiments

Female 5-week-old Balb/c-nude mice weighing approximately 15–20 g were used (All provided by Beijing Vital River Laboratory

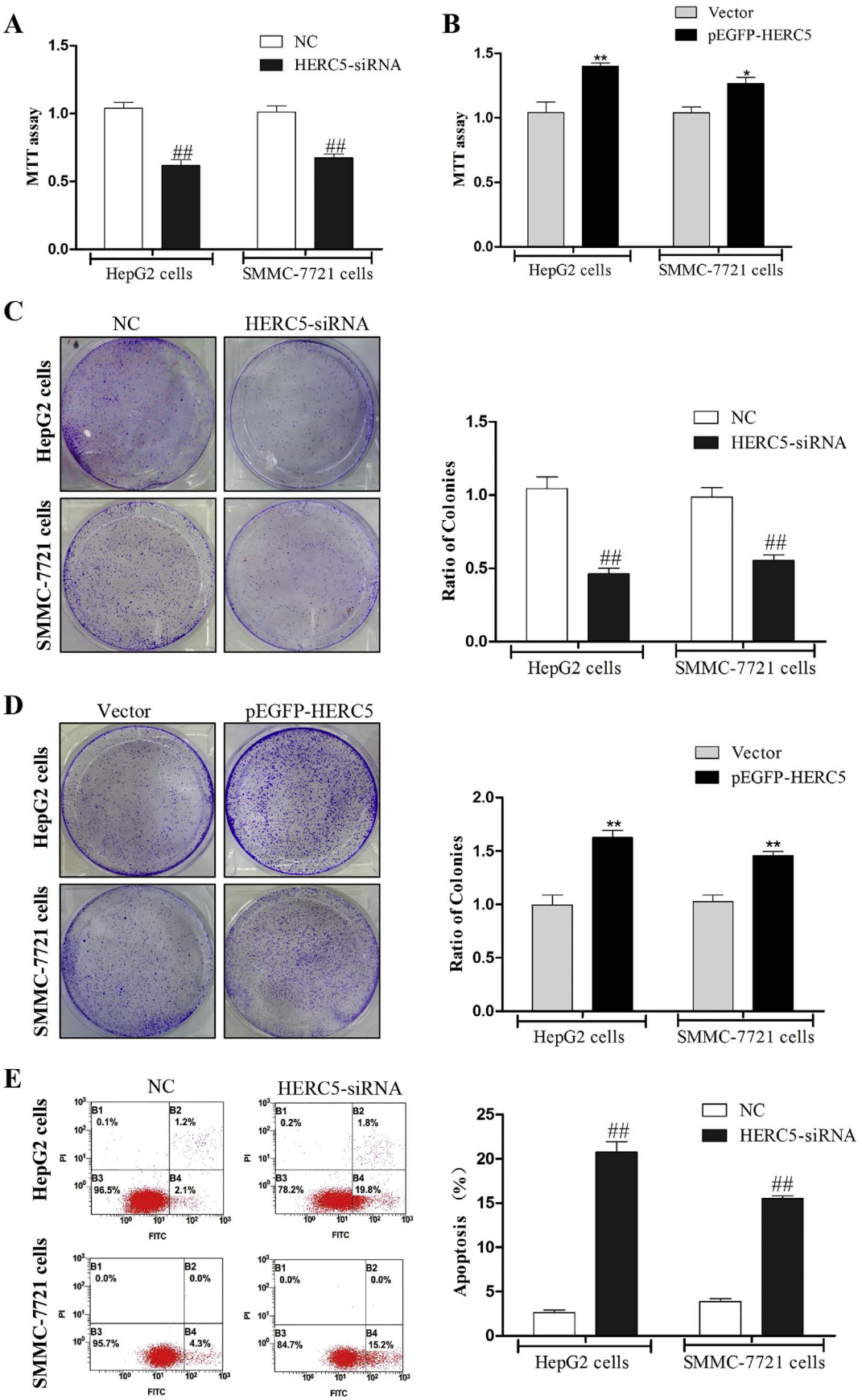

Fig. 2. HERC5 promotes HCC cell growth in vitro. (A–B) Cell growth of HepG2 and SMMC-7721 cells was determined after transfection with HERC5-siRNA or pEGFP-HERC5 by using MTT assay. (C–D) The single cell proliferation of HepG2 and SMMC-7721 cells was assessed after transfection with HERC5-siRNA or pEGFP-HERC5 by using colony forming assay. (E) Apoptosis was detected by Flow cytometry in HepG2 and SMMC-7721 cells with HERC5-siRNA transfection. $\#p < 0.05$ or $\#\#p < 0.01$ compared with NC group. NC: Negative control. $*p < 0.05$ or $**p < 0.01$ compared with Vector group. Data are represented as mean ± SD for three independent experiments.

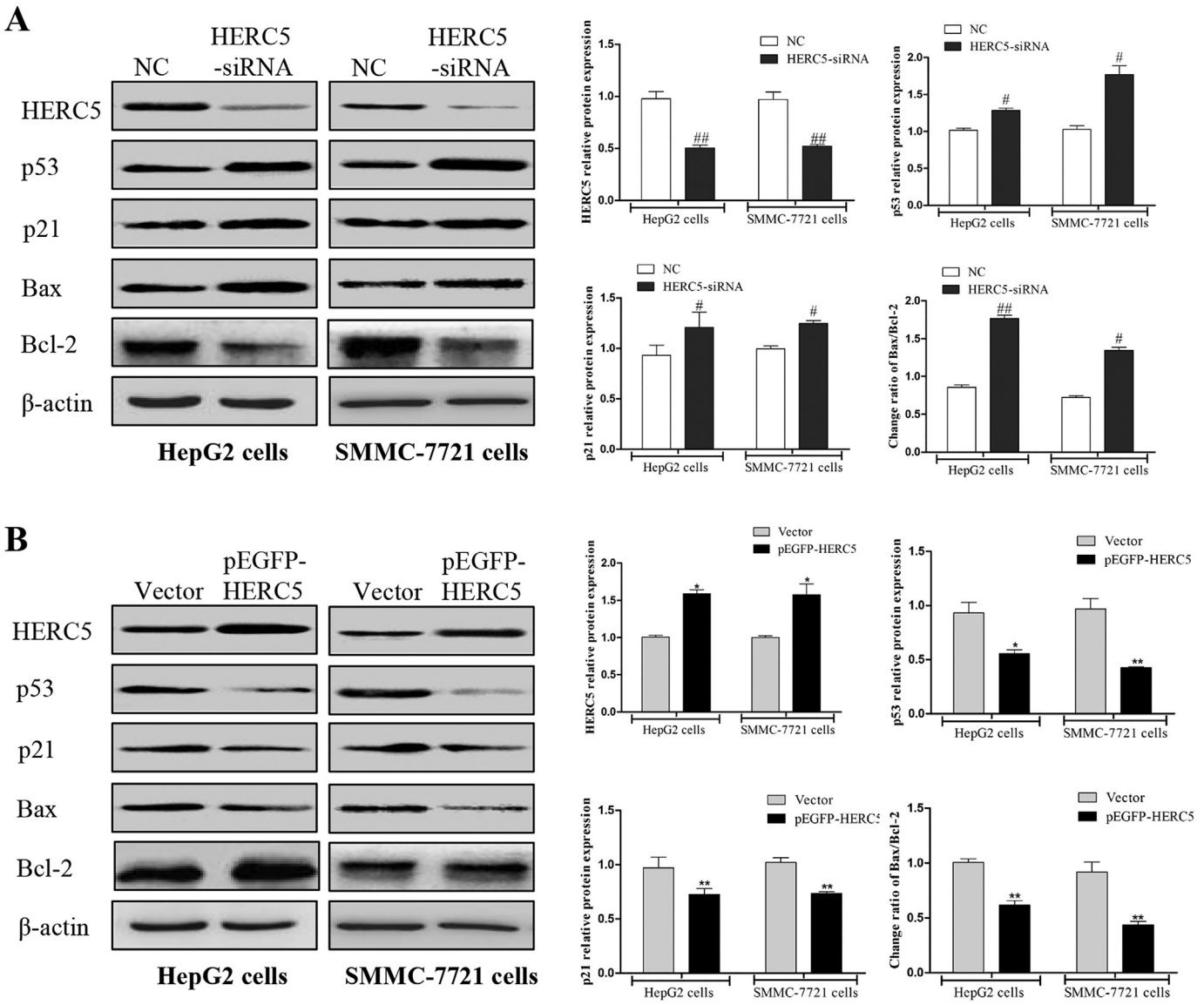

Fig. 3. The expression of p53 and its targets was measured in HERC5 down- or up-regulated HCC cells. (A) The protein expressions of p53, p21 and Bax/Bcl-2 after transfection with HERC5-siRNA were analyzed using Western blot. #$p < 0.05$ or ##$p < 0.01$ compared with NC group. (B) Over-expression of HERC5 decreased the protein expressions of p53, p21 and Bax/Bcl-2 in HepG2 and SMMC-7721. *$p < 0.05$ or **$p < 0.01$ compared with Vector group. Data are represented as mean ± SD for three independent experiments.

Animal Technology Co., Ltd.) and feed under specific pathogen-free conditions. To inject SMMC-7721 cells (1×10^7 resuspended in PBS/mice) subcutaneously into the dorsal sides of the mice. After a week, when tumors reached about 80–120 mm^3, the mice were grouped (8 mice per group) and injected intraperitoneally into mice daily with three doses of HZ-6d and doxorubicin (doxorubicin was used as a positive control). Control group mice were given the vehicle only. Tumors size was measured daily for 3 days. The tumors were calculated according to a formula: tumor volume = d2 × D/2. After 3 week, the mice were sacrificed and tumors were removed for the further research. The experimental procedures were approved by the University Animal Care and Use Committee.

2.14. Histopathology and immunohistochemical staining

The tumor specimens were fixed in 4% PFA immediately for 24 h and embedded in paraffin blocks. Processed for histological examination according to a standard procedure, and then stained with hematoxylin and eosin (H & E). To observe the changes of pathology and photographed by light microscope (Olympus, Japan).

Immunohistochemical (IHC) staining was performed in paraffin sections according to the manufacture's instruction. The sections were incubated with the primary antibodies overnight at 4 °C. After incubation in secondary antibody and 3, 3′-diaminoben-zidine (DAB substrate kit, ZSGB-BIO), and the slides were counterstained with hematoxylin, dehydrated, and mounted. The slides were visualized through light microscope (Olympus, Japan).

2.15. Statistical analysis

Data are presented as mean ± SD of all replicates and analyzed using SPSS16.0 software. Statistical analysis was performed by two-tailed unpaired *t*-test or one-way ANOVA. In all cases, p value < 0.05 was considered to be statistically significant.

3. Results

3.1. HERC5 and ISG15 are highly expressed in HCC tissues and cell lines

HERC5 and ISG15 expression were measured in HCC tissues

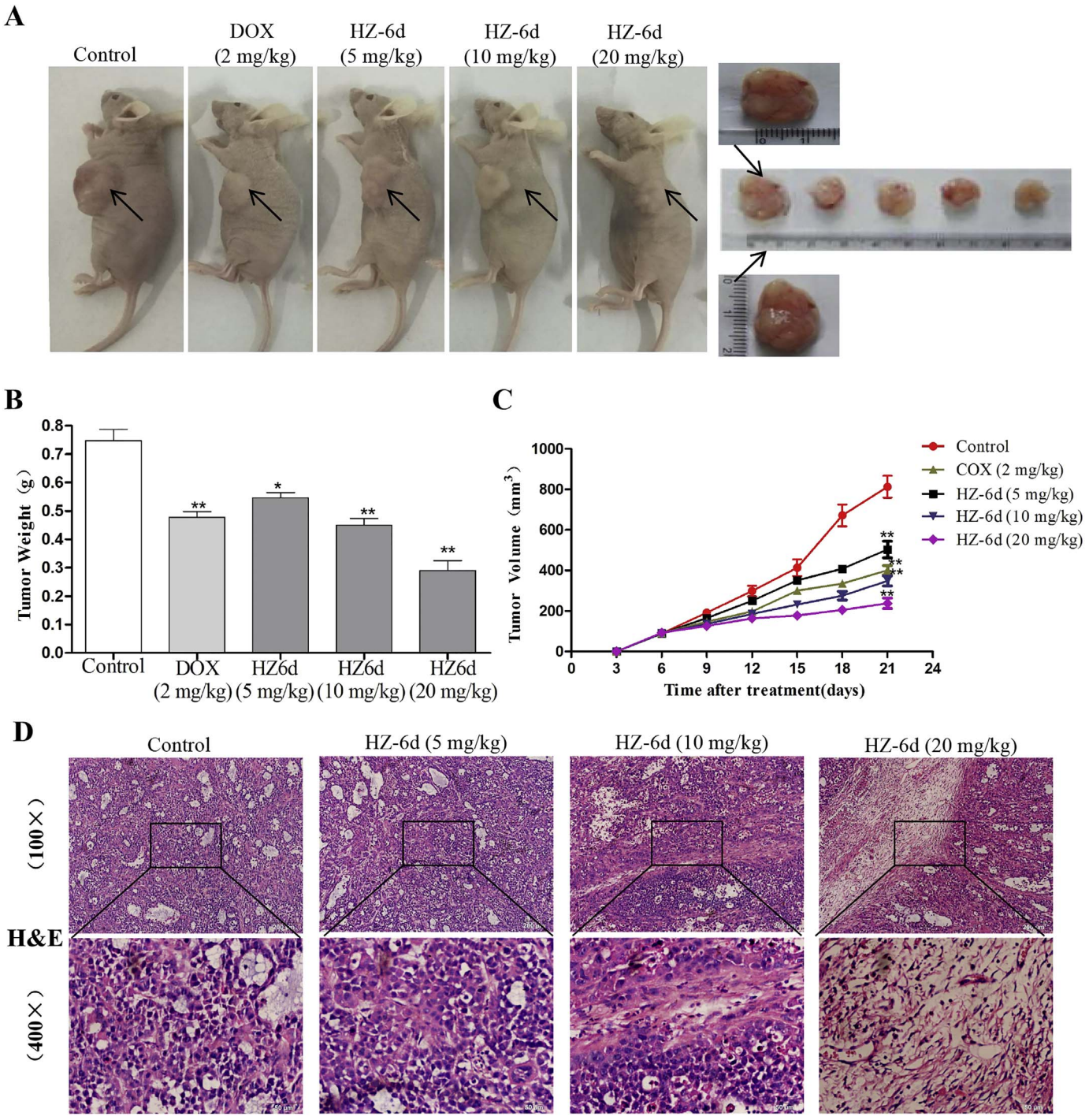

Fig. 4. HZ-6d inhibited tumor growth in nude mouse model. (A) SMMC-7721 cells were subcutaneously injected into 5-week-old mice to generate tumors and treated with different concentrations of HZ-6d. Tumors in HZ-6d treated groups were smaller than in untreated groups ($n = 8$ mice in each group). (B–C) Effects of HZ6d on tumor volume and weight compared with control groups. *$p < 0.05$ or **$p < 0.01$. (D) Effects of HZ-6d on tumor histopathology stained with H & E (100 × and 400 × magnification).

compared to non-tumor counterparts. Quantitative real-time PCR, Immunohistochemical and Western bolt analysis revealed that the mRNA and protein levels of HERC5 and ISG15 in HCC tissues were much higher compared to adjacent tissues (Fig. 1A–C). Next, we measured whether HERC5 and ISG15 over-expressed in HepG2 and SMMC-7721 cells with a non-HCC cell line L-02 as control. The results are in agreement with the above (Fig. 1D and E). We found that HERC5 and ISG15 were over-expressed in human tissues and HepG2 and SMMC-7721 cells.

3.2. HERC5 promotes cancerous proliferation and involves in cell apoptosis

The functional role of HERC5 in HCC was further detected. MTT assay was performed to test the effect of HERC5 on cell proliferation. Knockdown of HERC5 by siRNA in HepG2 and SMMC-7721 cells exhibited lower proliferation rate than the negative control groups (Fig. 2A). In contrast, HERC5 over-expression showed a much higher viability compared with the cells transfected with Vector (Fig. 2B). Similarly, colony formation was suppressed by silencing of HERC5 in

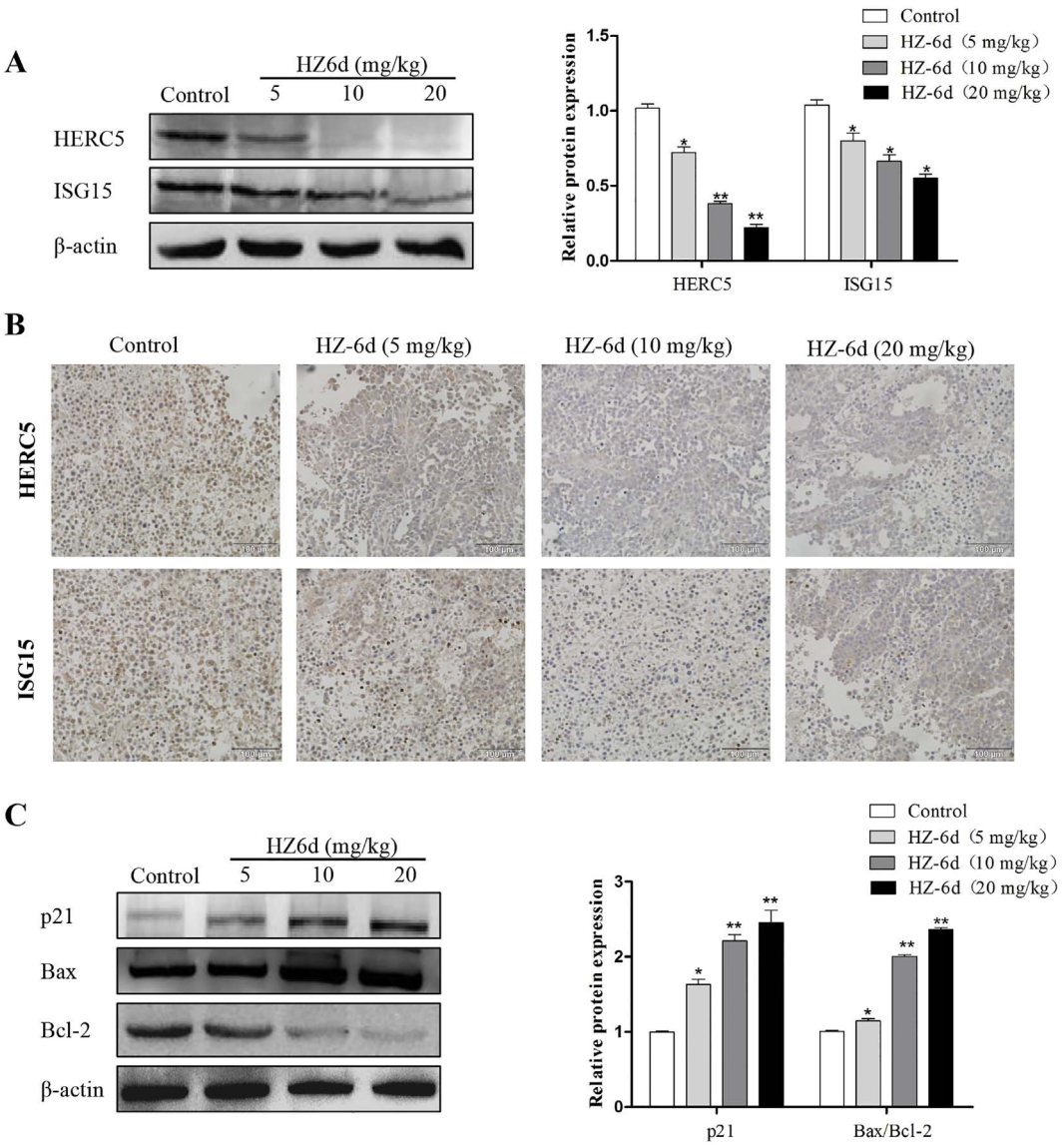

Fig. 5. Changes of HERC5, ISG15 and p53 related protein expression in xenograft tumors. (A–B) The tumor tissues treated with HZ-6d were examined to the expression of HERC5 and ISG15 by Western blot and Immunohistochemical analysis. (C) The expression of p21, Bax and Bcl-2 were detected by Western blot analysis. $*p < 0.05$ or $**p < 0.01$ compared with control group. Data are represented as mean ± SD for three independent experiments.

both HepG2 and SMMC-7721 cells (Fig. 2C). Not interestingly, up-regulation of HERC5 promoted colony formation in both HepG2 and SMMC-7721 cells (Fig. 2D). We next evaluated the effect of HERC5 using flow cytometry. The results showed that reduced expression of HERC5 significantly increased cell apoptosis (Fig. 2E), suggesting that HERC5 is implicated in tumor progression of HCC.

3.3. HERC5 is associated with p53-mediated pathway in HCC

Then we investigated a potential mechanism for HERC5 mediated HCC cell growth. It is well established that the level of p53 gene is normally down-expression or deficient in HCC. The HERC5 level was negatively correlated with p53 expression, silencing of HERC5 remarkably increased the protein level of p53, p21 and Bax/Bcl-2 in HepG2 and SMMC-7721 cells (Fig. 3A). More importantly, we detected that over-expression of HERC5 led to lower expression of p53, p21 and Bax/Bcl-2 in HepG2 and SMMC-7721 cells (Fig. 3B). These finding revealed that HERC5 mediated proliferation and apoptosis may be via inactivation of p53 in HCC cells.

3.4. HZ-6d tended to bind and stabilize the HERC5 G-quadruplex

HZ-6d was synthesized by our group and its structure as shown in (Supplementary Fig. 1A). The stability of the interaction between HZ-6d and HERC5 gene G-quadruplex was elucidated using molecular docking, and CD spectroscopy assay. The interaction between HZ-6d and the HERC5 gene G-quadruplex was elucidated using molecular docking experiment. We used a quadruplex main body and HERC5 G-rich sequence d (AGGGGGGAGGGAGGGTGG) oligonucleotide for large-molecule docking. Molecular docking results showed that HZ-6d tended to bind the G-quartet with classic π-π stacking interaction (Supplementary Fig. 1C, D). And the two side chains were extended to groove from the tetrad plane. The CD spectrum of the randomized d oligonucleotide appeared a negative band at 240 nm and a major positive band at 260 nm, and, with the increased of HZ-6d concentration from 1 to 5 Mol equivalence, the positive peak gradually increased at around 260 nm, and the negative band also increased at around 240 nm (Supplementary Fig. 1B). These results revealed that compound HZ-6d could bind and stabilize the HERC5 G-quadruplex structure and inhibition of the G-rich sequence expression.

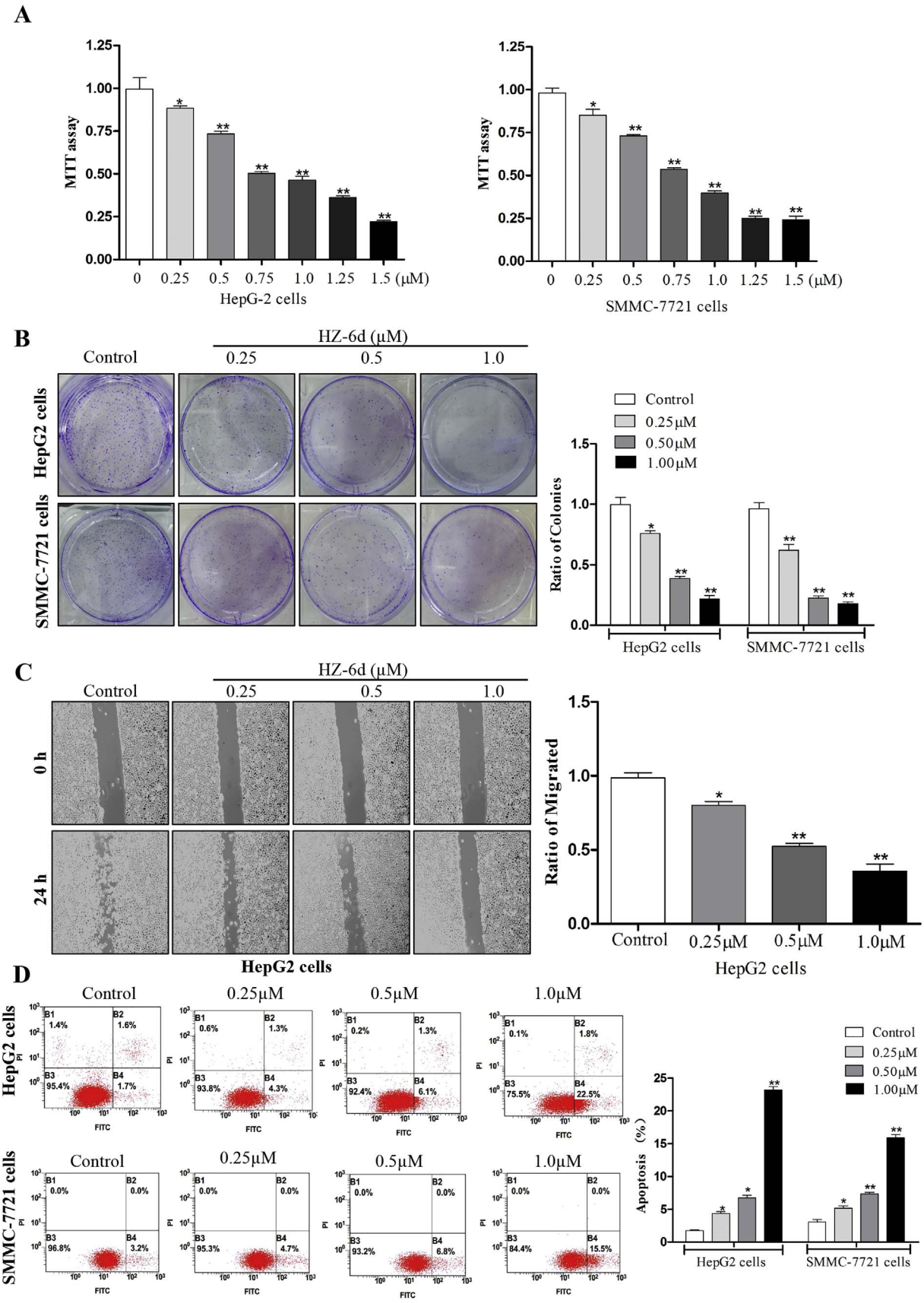

Fig. 6. Effects of HZ-6d on cell growth, migration and apoptosis. (A) MTT was used to detect the effect of HZ6d on cell proliferation. (B) Incubation with HZ-6d effectively inhibits colony formation. (C) The wound-healing assay was used to analyze the cell migration in HepG2 cells after different concentration HZ-6d treatment. (D) Flow cytometry analyzed the apoptotic cells exposed to different concentrations of HZ-6d for 24 h. $*p < 0.05$ or $**p < 0.01$ compared with control group. Data are represented as mean ± SD for three independent experiments.

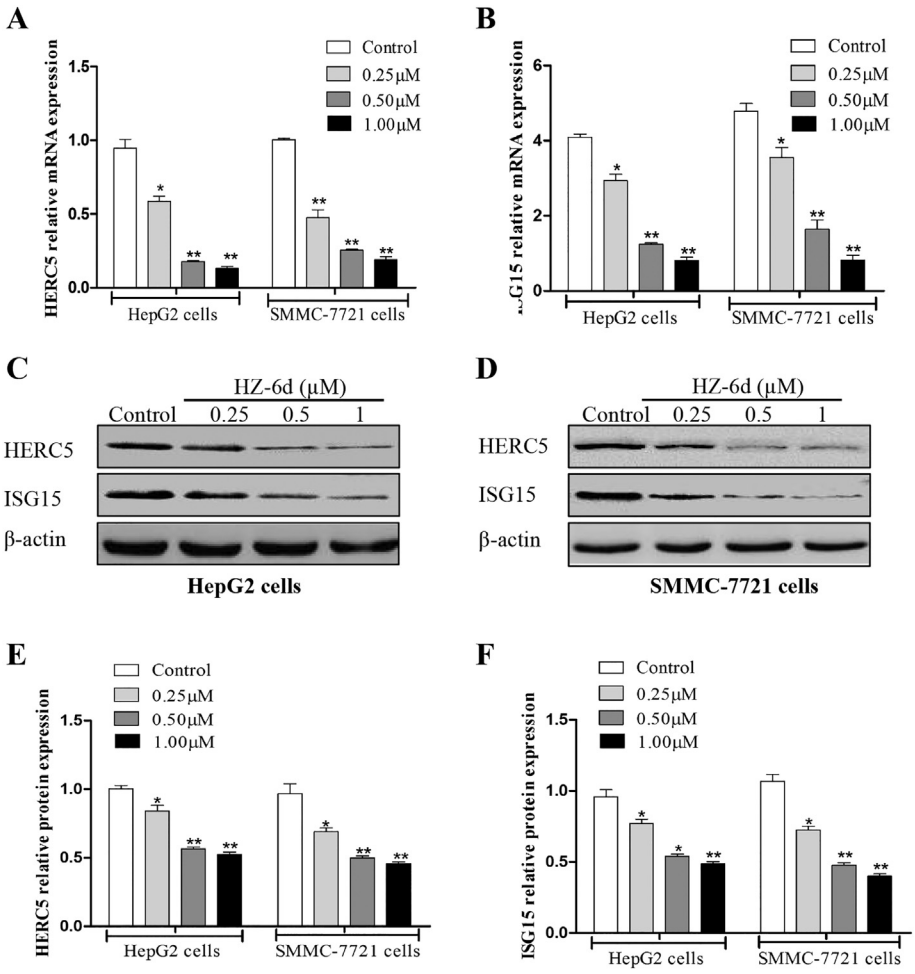

Fig. 7. HZ-6d down-regulate HERC5 and ISG15 expression in HCC cells. (A–B) The HERC5 and ISG15 mRNA expression were determined in HepG2 and SMMC-7721 cells treated with HZ-6d. (C–F) Expression of HERC5 and ISG15 proteins were detected in HepG2 and SMMC-7721 cells with HZ-6d. $*p < 0.05$ or $**p < 0.01$ compared with control group. Data are represented as mean ± SD for three independent experiments.

3.5. HZ-6d effectively delayed HCC growth and decreased HERC5 and ISG15 expression in vivo

We evaluated antitumor effects of HZ-6d as demonstrated in vivo within nude mice bearing SMMC-7721 xenografts. As compared with non-HZ-6d treated group (control group), at doses of 5, 10, and 20 mg/kg, the growth of SMMC-7721 xenografts was effectively restrained by 26.7%, 38.7%, and 61.3%, respectively. Doxorubicin (2 mg/kg) restrained the growth of SMMC-7721 xenografts by 36.0% (Fig. 4A–B and Supplementary Table 3). Tumor volumes were measured every three days after implantation. For a valid scientific outcome, we ensure that the size of any tumors did not exceed the 1.5 cm in this study (Workman et al., 2010). Our data showed that the volumes of tumor in the HZ-6d groups were significantly smaller as compared to control group at the late experimental stage (Fig. 4C). The separation of nude mice tumor nodules are round, oval, or irregular shape. H & E staining showed that the control group cells arranged densely in funicular, the nuclei volume will enlarge, and dark dye. Compared with the control group, we found in different degrees of cells shrinkage, or nuclear condensation and more spaces between the cells in the three doses of HZ-6d treatment groups (Fig. 4D). Immunohistochemical and Western blot demonstrated that HZ-6d down-regulated the HERC5 and ISG15 protein level in xenografts tumors (Fig. 5A and B). More interestingly, Western blot detected that HZ-6d also increased the expression of p21 and the ratio of Bax/Bcl-2 (Fig. 5C). These data together demonstrated that HZ-6d treatment effectively inhibited tumor growth in vivo and blocked the expression of HERC5 and ISG15, resulting the activation of p53 related gene.

3.6. HZ-6d treatment suppressed the growth of HCC cells and down-regulated HERC5 and ISG15 expression in vitro

To investigate whether HZ-6d treatment suppress cell growth on HCC cells, MTT assay used to measure the growth viability in HepG2 and SMMC-7721 cells treated with various concentrations of HZ-6d for 24 h, respectively. The results showed significantly effect of HZ-6d in both HepG2 and SMMC-7721 cells (Fig. 6A). The inhibitory concentration (IC50) in the 24 h exposure time for HepG2 and SMMC-7721 were 0.94 ± 0.22 μM and 0.93 ± 0.09 μM, respectively. We found that the colony forming abilities of HepG2 and SMMC-7721 cells were effectively suppressed by HZ-6d (Fig. 6B). Moreover, our wound healing assay demonstrated that HZ-6d significantly decreased cell migration in both HepG2 and SMMC-7721 cells (Fig. 6C). Flow cytometry analysis detected that HZ-6d treatment significantly increases in the percentage of apoptosis in HepG2 and SMMC-7721 cells (Fig. 6D). We measured the expression of HERC5 and ISG15 at mRNA and protein levels in HCC cells treated with HZ-6d. Quantitative real-time PCR analysis result demonstrated that HERC5 and ISG15 mRNA level were markedly decreased in HepG2 and SMMC-7721 cells after HZ-6d treatment (Fig. 7A and B). Western blot analysis further verified that HZ-6d treatment silenced HERC5 and ISG15 expressions in HepG2 and SMMC-7721 cells (Fig. 7C–F). In general, our data indicated that the treatment of HZ-6d is associated with the decreased proliferation and migration of HCC cells, which may be dependent on the inactivation of HERC5 and ISG15.

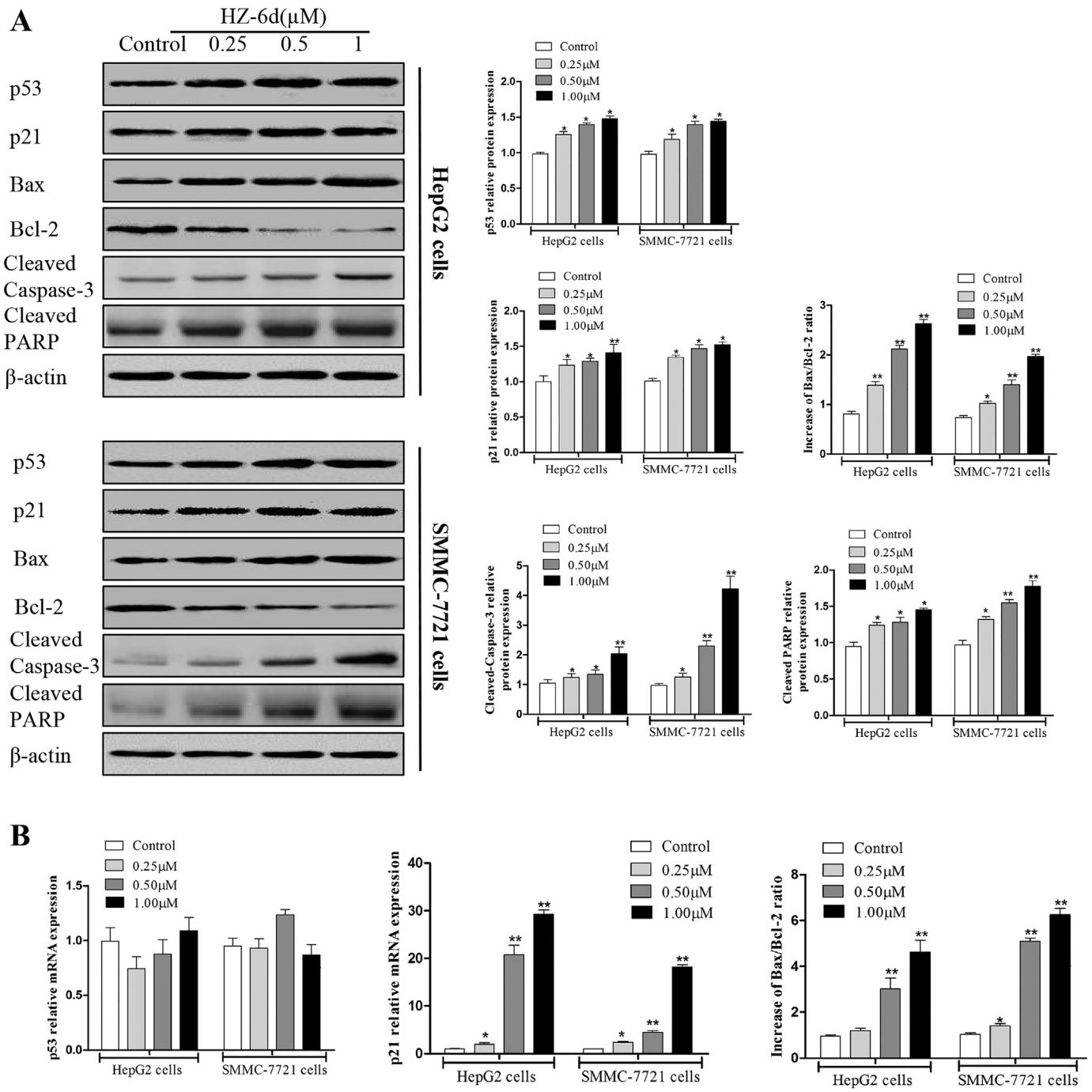

Fig. 8. HZ-6d up-regulated p53 and p53 target genes expression. (A) Successively, protein expression of p53, p21, Bax/Bcl2, Cleaved-Caspase-3 and Cleaved PARP were examined by Western blot analysis. (B) The p53, p21 and Bax/Bcl-2 mRNA expression was detected in HCC cells treated with HZ-6d. *$p < 0.05$ or **$p < 0.01$ compared with control group. Data are represented as mean ± SD for three independent experiments.

3.7. HZ-6d reactivated the p53-mediated pathway in HCC

There are evidences that HERC5 has an association with the ISG15-dependent p53 degradation (Huang and Bulavin, 2014; Huang et al., 2014). To investigate whether HZ-6d influences the p53 pathway, HepG2 and SMMC-7721 cells were treated with HZ-6d for different concentrations. Our Western blot analysis found that p53, p21, Cleaved-Caspase-3, Cleaved PARP and the ratio of Bax/Bcl-2 protein levels were markedly increased in HepG2 and SMMC-7721 cells (with wild-type p53) by HZ-6d treatment (Fig. 8A). Likewise, Quantitative real-time PCR showed that p21 and Bax/Bcl-2 mRNA levels were up-regulated by HZ-6d in HepG2 and SMMC-7721 cells. However, there was no difference in p53 mRNA level between control and treatment groups (Fig. 8B). These results supported our observation that the activation of p53 by compound HZ-6d regulated might through the posttranscriptional modification.

3.8. Down-regulation of HERC5 by siRNA increased HZ-6d-induced p53 protein accumulation

To further investigate the related mechanism of HZ-6d in HCC, siRNA specific for human HERC5 was used to knockdown the HERC5 expression. Our results revealed that down-regulation of HERC5 could reactivate p53, p21 and Bax/Bcl-2 and the trend is the same as the

treatment of HZ-6d. Consistently, down-regulation of HERC5 in combination with HZ-6d treatment induced p53, p21 and Bax/Bcl-2 expression to more degree compared with HZ-6d alone or siRNA treatment alone (Supplementary Fig. 2). These data provide evidence that HZ-6d exhibits anti-tumor activity through regulation of HERC5 and its target protein p53.

4. Discussion

Studies have shown that chronic infection with either hepatitis B virus (HBV) or hepatitis C virus (HCV), excessive alcohol intake and dietary aflatoxin exposure are common risk factors for HCC (Bruix et al., 2011; Lee et al., 2013; Tseng and Kao, 2017). Now, evidence has emerged that the development of HCC is a multiple steps, multiple phases procession, which involved in activation of multiple proto-oncogenes and inactivation of tumor suppressor genes. Among these altered genes, p53 is a significant one (Yonish-Rouach et al., 1991; Zuckerman et al., 2009; Bieging et al., 2014; Li et al., 2016a; Charni et al., 2017).

The activity of p53 proteins are tightly regulated by a large number of posttranslational modifications, including sumoylation, acetylation and ubiquitinatio (Rodriguez et al., 1999; Brooks and Gu, 2011; Nihira et al., 2017). These modifications are critical for the activity and function of p53 protein. Recently, it has been reported that ISG15 can be conjugated to p53 and this modification promotes the degradation of p53. Encouragingly, HERC5 is a primary E3 ligase of ISG15-modifying, and it has been shown to play a vital role in broad targeting of many proteins, potentially including p53. However, little information is available to us on the expression of HERC5 and its extra functions in HCC. This study suggested that HERC5 and ISG15 are increased in both HCC tissue samples and cell lines relative to their respective normal counterparts. Silencing expression of HERC5 significantly suppressed cell proliferation, induced apoptosis in HCC cells. Conversely, enforced over-expression of HERC5 exhibited opposite results. Importantly, we showed that the mechanism of by which silence of HERC5 inhibits HCC cell growth is attributable to the activation of p53 pathway.

The G-quadruplex DNA is widely discovered in human gene promoters which attracted extensive attention (Duchler, 2012; Kendrick et al., 2017). Inspired by the approach to develop bioavailable small molecule ligands interacting with the G-quadruplex, we screened some disubstituted quinazoline derivatives, which binds HERC5 G-rich sequence directly and induces a structure formation in G-quadruplex that blocks double-stranded DNA replication. Our initial work in HepG2, SMMC-7721 and BEL-7402 cells indicated that the 7, 11-disubstituted quinazoline derivative HZ-6d had stronger anti-cancer activity than others (data not shown). Therefore, we used HZ-6d in the following studies. In order to understand the interaction between HZ-6d and HERC5, molecular modeling studies were carried out. It was proved that molecular docking of HZ-6d was performed on the binding model based on the HERC5 G-quadruplex structure. Along with CD spectroscopy, our results demonstrated that the compound could binds and stabilizes the HERC5 G-quadruplex. Furthermore, we used HCC cells and nude mice xenografts to study the anti-tumor effects of HZ-6d. Experimental results showed that treatment with HZ-6d caused a significant inhibition of cell proliferation and migration in HepG2 and SMMC-7721 cells. Equally, the tumor suppressive effect of HZ-6d on HCC growth was also confirmed in nude mice xenografts. Our results demonstrated the fact that HZ-6d might effectively inhibit the growth of HCC in vitro and vivo.

To further understand the anti-cancer mechanism of HZ6d, examined the expression of HERC5 and ISG15. In this study, HZ6d was found to reduce the expression of HERC5 and ISG15 in HCC cell lines and xenografts tumors. As a transcription factor, p53 plays a multiple and important role in cells to maintain genetic stability and function, including cell proliferation, apoptosis, and many other cellular processes (Yoon et al., 2015). Interestingly, HZ6d treatment given rise to the accumulation of p53 protein not mRNA. The activated of p53 then binds to the p53-responsive element (p53 RE) results in p53-dependent transcriptional activity and apoptosis of tumor cells, including the cell cycle regulator gene p21 and pro-apoptotic gene Bax (Wu et al., 2008; Hawkes and Alkan, 2011). Western blot analysis also showed that HZ-6d significantly induced changes in p21, Bax/Bcl-2, supporting that the activation of p53-mediated pathway. Meanwhile, Cleaved-Caspase-3 expression was up-regulated significantly by treatment with HZ-6d may also be involved in the p53 activate apoptotic pathway, which directly induces mitochondrial membrane permeabilization and apoptosis (Chipuk et al., 2004; Liu et al., 2016). HZ-6d also significantly increased the expression levels of Cleaved PRAP (Si et al., 2017; Tao et al., 2017). Concordantly, our data demonstrated that knockdown of HERC5 by transfecting siRNA increased HZ-6d-induced p53 and its downstream genes p21 and Bax/Bcl-2 expression in HepG2 and SMMC-7721 cells. Based on the experimental data discussed above, we conclude that HZ-6d interacts with HERC5, preventing HERC5 and p53 protein interaction, thereby keeping p53 from ISG15-dependent degradation pathway.

In conclusion, our studies determined that HERC5 may play an important role in HCC. HZ-6d possessed high effectiveness in the inhibition of HCC growth was due to block the HERC5 double-stranded DNA replication, suppressed HERC5 expression. Accordingly, the decreased of HERC5 induced p53 protein accumulation through inhibited ISGylation mediated p53 degradation pathway. Therefore, HERC5 might be an attractive target for drug discovery and HZ-6d could be developed as a lead compounds for treatment of HCC.

Supplementary data to this article can be found online at http://dx.doi.org/10.1016/j.taap.2017.09.011.

Conflict of interest

All authors declared no conflict of interest in this article.

Acknowledgments

This study was supported by the Intercollegiate Key Projects of Nature Science of Anhui Province (KJ2017A169) and key Research Foundation of Higher Education of Anhui Province (gxfx2017011).

References

Abdelsalam, M.E., Murthy, R., Avritscher, R., Mahvash, A., Wallace, M., Kaseb, A., Odisio, B., 2016. Minimally invasive image-guided therapies for hepatocellular carcinoma. J. Hepatocell. Carcinoma **3**, 55–61.
Adrian, M., Ang, D.J., Lech, C.J., Heddi, B., Nicolas, A., Phan, A.T., 2014. Structure and conformational dynamics of a stacked dimeric G-quadruplex formed by the human CEB1 minisatellite. J. Am. Chem. Soc. 136, 6297–6305.
Alisi, A., Balsano, C., 2007. Enhancing the efficacy of hepatocellular carcinoma chemotherapeutics with natural anticancer agents. Nutr. Rev. 65, 550–553.
Au, J.S., Frenette, C.T., 2015. Management of hepatocellular carcinoma: current status and future directions. Gut Liver 9, 437–448.
Balogh, J., Victor, D., Asham, E.H., Burroughs, S.G., Boktour, M., Saharia, A., Li, X., Ghobrial, R.M., Monsour Jr., H.P., 2016. Hepatocellular carcinoma: a review. J. Hepatocell. Carcinoma 3, 41–53.
Bieging, K.T., Mello, S.S., Attardi, L.D., 2014. Unravelling mechanisms of p53-mediated tumour suppression. Nat. Rev. Cancer 14, 359–370.
Brooks, C.L., Gu, W., 2011. p53 regulation by ubiquitin. FEBS Lett. 585, 2803–2809.
Bruix, J., Sherman, M., American Association for the Study of Liver, D, 2011. Management of hepatocellular carcinoma: an update. Hepatology 53, 1020–1022.
Burge, S., Parkinson, G.N., Hazel, P., Todd, A.K., Neidle, S., 2006. Quadruplex DNA: sequence, topology and structure. Nucleic Acids Res. 34, 5402–5415.
Cajee, U.F., Hull, R., Ntwasa, M., 2012. Modification by ubiquitin-like proteins: significance in apoptosis and autophagy pathways. Int. J. Mol. Sci. 13, 11804–11831.
Chacko, S., Samanta, S., 2016. Hepatocellular carcinoma: a life-threatening disease. Biomed Pharmacother 84, 1679–1688.
Charni, M., Aloni-Grinstein, R., Molchadsky, A., Rotter, V., 2017. p53 on the crossroad between regeneration and cancer. Cell Death Differ. 24, 8–14.
Chen, F., Wang, W., El-Deiry, W.S., 2010. Current strategies to target p53 in cancer. Biochem. Pharmacol. 80, 724–730.
Cherqui, D., 2015. Laparoscopic liver resection: a new paradigm in the management of hepatocellular carcinoma? J. Hepatol. 63, 540–542.
Chipuk, J.E., Kuwana, T., Bouchier-Hayes, L., Droin, N.M., Newmeyer, D.D., Schuler, M., Green, D.R., 2004. Direct activation of Bax by p53 mediates mitochondrial membrane

permeabilization and apoptosis. Science 303, 1010–1014.
Darb-Esfahani, S., Sinn, B.V., Rudl, M., Sehouli, J., Braicu, I., Dietel, M., Denkert, C., 2014. Interferon-stimulated gene, 15 kDa (ISG15) in ovarian high-grade serous carcinoma: prognostic impact and link to NF-kappaB pathway. Int. J. Gynecol. Pathol. 33, 16–22.
Dastur, A., Beaudenon, S., Kelley, M., Krug, R.M., Huibregtse, J.M., 2006. Herc5, an interferon-induced HECT E3 enzyme, is required for conjugation of ISG15 in human cells. J. Biol. Chem. 281, 4334–4338.
Desai, S.D., 2015. ISG15: a double edged sword in cancer. Oncoimmunology 4, e1052935.
Desai, S.D., Wood, L.M., Tsai, Y.C., Hsieh, T.S., Marks, J.R., Scott, G.L., Giovanella, B.C., Liu, L.F., 2008. ISG15 as a novel tumor biomarker for drug sensitivity. Mol. Cancer Ther. 7, 1430–1439.
Duchler, M., 2012. G-quadruplexes: targets and tools in anticancer drug design. J. Drug Target. 20, 389–400.
Hawkes, W.C., Alkan, Z., 2011. Delayed cell cycle progression from SEPW1 depletion is p53- and p21-dependent in MCF-7 breast cancer cells. Biochem. Biophys. Res. Commun. 413, 36–40.
Huang, Y.F., Bulavin, D.V., 2014. Oncogene-mediated regulation of p53 ISGylation and functions. Oncotarget 5, 5808–5818.
Huang, Y.F., Wee, S., Gunaratne, J., Lane, D.P., Bulavin, D.V., 2014. Isg15 controls p53 stability and functions. Cell Cycle 13, 2200–2210.
Jemal, A., Bray, F., Center, M.M., Ferlay, J., Ward, E., Forman, D., 2011. Global cancer statistics. CA Cancer J. Clin. 61, 69–90.
Kendrick, S., Muranyi, A., Gokhale, V., Hurley, L.H., Rimsza, L.M., 2017. Simultaneous drug targeting of the promoter MYC G-quadruplex and BCL2 i-motif in diffuse large B-cell lymphoma delays tumor growth. J. Med. Chem.
Kim, K.I., Giannakopoulos, N.V., Virgin, H.W., Zhang, D.E., 2004. Interferon-inducible ubiquitin E2, Ubc8, is a conjugating enzyme for protein ISGylation. Mol. Cell. Biol. 24, 9592–9600.
Lai, C., Struckhoff, J.J., Schneider, J., Martinez-Sobrido, L., Wolff, T., Garcia-Sastre, A., Zhang, D.E., Lenschow, D.J., 2009. Mice lacking the ISG15 E1 enzyme UbE1L demonstrate increased susceptibility to both mouse-adapted and non-mouse-adapted influenza B virus infection. J. Virol. 83, 1147–1151.
Lee, M.H., Yang, H.I., Liu, J., Batrla-Utermann, R., Jen, C.L., Iloeje, U.H., Lu, S.N., You, S.L., Wang, L.Y., Chen, C.J., Group, R.E.V.E.A.L.H.S, 2013. Prediction models of long-term cirrhosis and hepatocellular carcinoma risk in chronic hepatitis B patients: risk scores integrating host and virus profiles. Hepatology 58, 546–554.
Levine, A.J., 1997. p53, the cellular gatekeeper for growth and division. Cell 88, 323–331.
Li, Z., Tan, J.H., He, J.H., Long, Y., Ou, T.M., Li, D., Gu, L.Q., Huang, Z.S., 2012. Disubstituted quinazoline derivatives as a new type of highly selective ligands for telomeric G-quadruplex DNA. Eur. J. Med. Chem. 47, 299–311.
Li, C., Wang, J., Zhang, H., Zhu, M., Chen, F., Hu, Y., Liu, H., Zhu, H., 2014. Interferon-stimulated gene 15 (ISG15) is a trigger for tumorigenesis and metastasis of hepatocellular carcinoma. Oncotarget 5, 8429–8441.
Li, Z., Liu, C., Huang, C., Meng, X., Zhang, L., He, J., Li, J., 2016a. Quinazoline derivative QPB-15e stabilizes the c-myc promoter G-quadruplex and inhibits tumor growth in vivo. Oncotarget 7, 34266–34276.
Li, T., Liu, X., Jiang, L., Manfredi, J., Zha, S., Gu, W., 2016b. Loss of p53-mediated cell-cycle arrest, senescence and apoptosis promotes genomic instability and premature aging. Oncotarget 7, 11838–11849.
Linzer, D.I., Levine, A.J., 1979. Characterization of a 54K dalton cellular SV40 tumor antigen present in SV40-transformed cells and uninfected embryonal carcinoma cells. Cell 17, 43–52.
Liu, C., Vojnovic, D., Kochevar, I.E., Jurkunas, U.V., 2016. UV-A irradiation activates Nrf2-regulated antioxidant defense and induces p53/Caspase3-dependent apoptosis in corneal endothelial cells. Invest. Ophthalmol. Vis. Sci. 57, 2319–2327.
Loeb, K.R., Haas, A.L., 1992. The interferon-inducible 15-kDa ubiquitin homolog conjugates to intracellular proteins. J. Biol. Chem. 267, 7806–7813.
Ma, D.L., Zhang, Z., Wang, M., Lu, L., Zhong, H.J., Leung, C.H., 2015. Recent developments in G-Quadruplex probes. Chem. Biol. 22, 812–828.
Muller, P.A., Vousden, K.H., 2014. Mutant p53 in cancer: new functions and therapeutic opportunities. Cancer Cell 25, 304–317.
Nihira, N.T., Ogura, K., Shimizu, K., North, B.J., Zhang, J., Gao, D., Inuzuka, H., Wei, W., 2017. Acetylation-dependent regulation of MDM2 E3 ligase activity dictates its oncogenic function. Sci. Signal. 10.
Polyak, K., Xia, Y., Zweier, J.L., Kinzler, K.W., Vogelstein, B., 1997. A model for p53-induced apoptosis. Nature 389, 300–305.
Rodriguez, M.S., Desterro, J.M., Lain, S., Midgley, C.A., Lane, D.P., Hay, R.T., 1999. SUMO-1 modification activates the transcriptional response of p53. EMBO J. 18, 6455–6461.
Roh, J.L., Ko, J.H., Moon, S.J., Ryu, C.H., Choi, J.Y., Koch, W.M., 2012. The p53-reactivating small-molecule RITA enhances cisplatin-induced cytotoxicity and apoptosis in head and neck cancer. Cancer Lett. 325, 35–41.
Si, L., Xu, L., Yin, L., Qi, Y., Han, X., Xu, Y., Zhao, Y., Liu, K., Peng, J., 2017. Potent effects of dioscin against pancreatic cancer via miR-149-3P-mediated inhibition of the Akt1 signalling pathway. Br. J. Pharmacol. 174, 553–568.
Tao, X., Xu, L., Yin, L., Han, X., Qi, Y., Xu, Y., Song, S., Zhao, Y., Peng, J., 2017. Dioscin induces prostate cancer cell apoptosis through activation of estrogen receptor-beta. Cell Death Dis. 8, e2989.
Tseng, T.C., Kao, J.H., 2017. HBV markers for HCC prediction: three heads are better than two? J. Hepatol.
Wong, J.J., Pung, Y.F., Sze, N.S., Chin, K.C., 2006. HERC5 is an IFN-induced HECT-type E3 protein ligase that mediates type I IFN-induced ISGylation of protein targets. Proc. Natl. Acad. Sci. U. S. A. 103, 10735–10740.
Workman, P., Aboagye, E.O., Balkwill, F., Balmain, A., Bruder, G., Chaplin, D.J., Double, J.A., Everitt, J., Farningham, D.A., Glennie, M.J., Kelland, L.R., Robinson, V., Stratford, I.J., Tozer, G.M., Watson, S., Wedge, S.R., Eccles, S.A., Committee of the National Cancer Research, I, 2010. Guidelines for the welfare and use of animals in cancer research. Br. J. Cancer 102, 1555–1577.
Wu, Y., Xing, D., Liu, L., Gao, B., 2008. Regulation of Bax activation and apoptotic response to UV irradiation by p53 transcription-dependent and -independent pathways. Cancer Lett. 271, 231–239.
Yonish-Rouach, E., Resnitzky, D., Lotem, J., Sachs, L., Kimchi, A., Oren, M., 1991. Wild-type p53 induces apoptosis of myeloid leukaemic cells that is inhibited by interleukin-6. Nature 352, 345–347.
Yoon, K.W., Byun, S., Kwon, E., Hwang, S.Y., Chu, K., Hiraki, M., Jo, S.H., Weins, A., Hakroush, S., Cebulla, A., Sykes, D.B., Greka, A., Mundel, P., Fisher, D.E., Mandinova, A., Lee, S.W., 2015. Control of signaling-mediated clearance of apoptotic cells by the tumor suppressor p53. Science 349, 1261669.
Yue, B., Zhang, Y.S., Xu, H.M., Zhao, C.R., Li, Y.Y., Qin, Y.Z., Wang, R.Q., Sun, D., Yuan, Y., Lou, H.X., Qu, X.J., 2013. Riccardin D-26, a synthesized macrocyclic bisbibenzyl compound, inhibits human hepatocellular carcinoma growth through induction of apoptosis in p53-dependent way. Cancer Lett. 328, 104–113.
Zuckerman, V., Wolyniec, K., Sionov, R.V., Haupt, S., Haupt, Y., 2009. Tumour suppression by p53: the importance of apoptosis and cellular senescence. J. Pathol. 219, 3–15.
Zuo, C., Sheng, X., Ma, M., Xia, M., Ouyang, L., 2016. ISG15 in the tumorigenesis and treatment of cancer: an emerging role in malignancies of the digestive system. Oncotarget 7, 74393–74409.